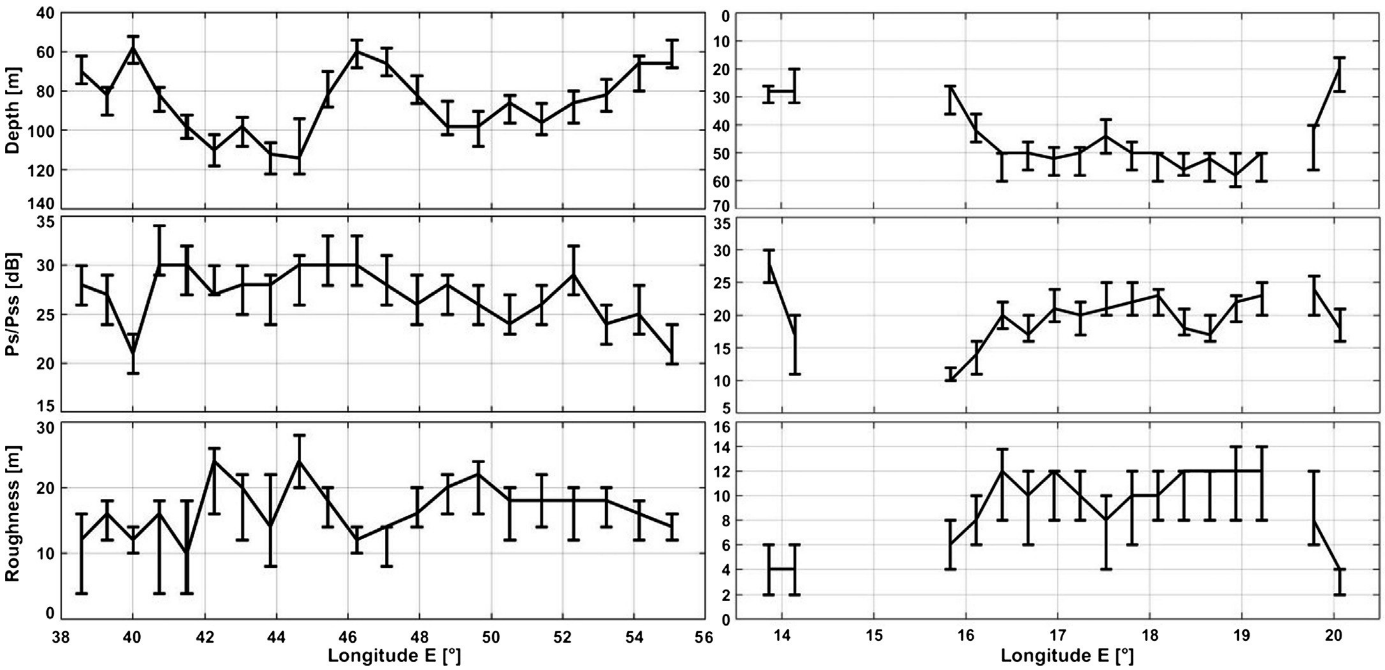

Fig. 3. Estimated depths (upper panels), surface-subsurface relative power (P_s/P_{ss}) (middle panels), and subsurface roughness (lower panels) for Punga Mare (left) and Baffin Sinus (right). Error bars are relative to 1-sigma uncertainty.

same qualitative considerations, the shallower bathymetry of North Kraken Mare at Baffin Sinus is also consistent with the morphology and brightness of this liquid body as observed from SAR images.

The depth of 110 m was measured at about 20–30 km from the nearest shoreline. This suggests a seabed profile that is rather steep, similar to that of the southern margin of Ligeia Mare as measured on T91 (Mastrogiuseppe et al., 2014a), and rather steeper than the northern part of that transect (160 m over ∼150 km). We note similarly that our bathymetric transect is at the southern margin of Punga Mare.

4. Seafloor backscattering: comparison of Punga and Ligeia Mare

In addition to the liquid composition, we use radar data for investigating dielectric properties of the seafloor. We compare seafloor backscattering of Punga Mare, observed during the T108, along with the backscattering of Ligeia Mare, measured using T91 flyby data. This comparison is particularly reliable since geometry and radar system parameters during the acquisition of the two observations were similar. We noted a remarkable similarity among echoes backscattered at the seafloor of the two seas, as shown with an example in Fig. 4. Radar waveforms indicate relative smooth topography (i.e. subsurface pulse shape approaches to a Gaussian single peak) and high transparency of the liquid (i.e. intensity ratio of surface and seafloor echoes is lower than 30 dB).

Considering the estimated specific attenuation K values of 13 dB/μs and 16 dB/μs for the Punga and Ligeia mare, respectively, we use formula (1) for a quantitative investigation of the sea floor composition of the two liquid bodies.

Formula (1) is used to relate the P_s/P_{ss} measurements with seafloor reflectivity R_{12}, surface reflectivity Γ_s, and attenuation K, assuming three possible values for the scattering term f_{ss}, which accounts for subsurface roughness scattering effects and can be expressed by rms slope. Such assumptions are necessary since the inversion problem is ill posed. For our study we derive the scattering terms f_{ss} using the Geometrical Optics (GO) formulation (Ulaby et al., 1982) along with three possible values of rms slopes ranging from 1° to 5°. Note that the rms slope values adopted here

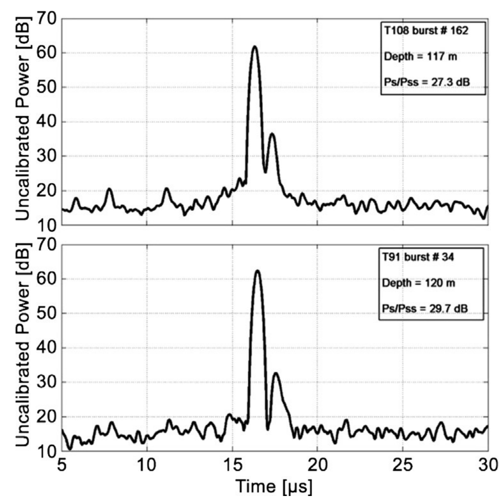

Fig. 4. Waveforms acquired during fly-by T108 over Punga (upper panel) and during fly-by T91 over Ligeia Mare (lower panel). Echoes backscattered from the seafloor are indicative of relative smooth topography at the resolution scale of the radar (35 m) and high transparency of the liquid.

are arbitrary and although they could represent the real values on Titan, they are only used in this study as reference values for comparing the dielectric properties of the two seafloors.

$$\left.\frac{P_s}{P_{ss}}\right|_{dB} = \Gamma_s|_{dB} - (1-\Gamma_s)^2\big|_{dB} - R_{12}|_{dB} + K|_{dB} + \left.\frac{f_s}{f_{ss}}\right|_{dB} \quad (1)$$

For each of the waveforms acquired over the two maria, inverting formula (1), we calculated a value of effective permittivity of the seafloor for different values of rms slope. The result is shown in Fig. 5 where the permittivity of the two seafloors is plotted along the radar transect of T91 and T108. We note that Ligeia Mare and Punga Mare seafloors show similar values of effective permittivity for similar values of small scale roughness. Moreover, the shape of radar waveforms suggests they have similar seafloor topography. Our conclusion is that the seafloors of both these maria are relatively smooth at the resolution scale of the radar (35 m)

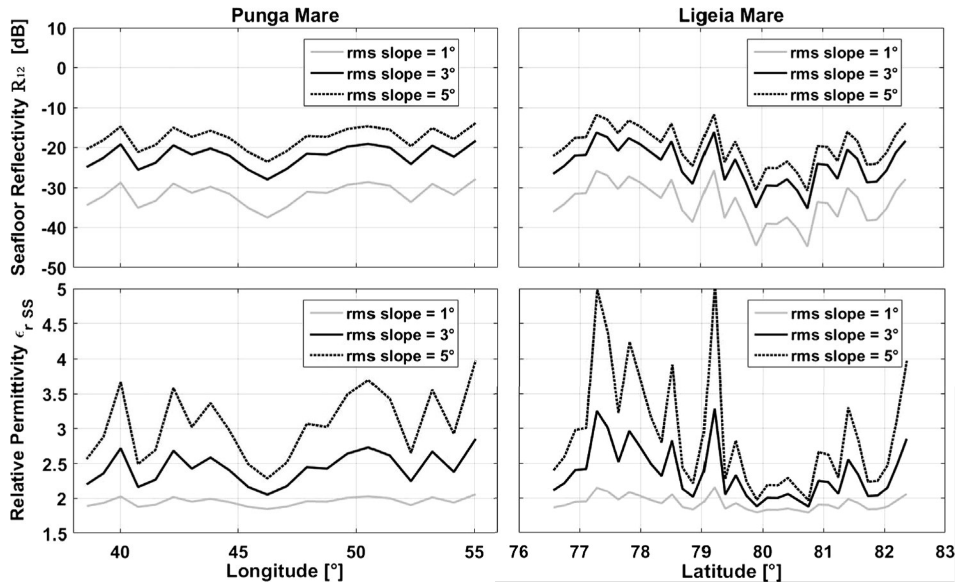

Fig. 5. Comparison between the seafloor reflectivity and the relative dielectric constant for Punga and Ligeia Mare for three possible values of rms slope. (Left column) Punga Mare. (Right column) Ligeia Mare.

and considering the adopted values for the microscale roughness, the composition of the two sea floors is consistent with several possible materials present on Titan, such as solid organics, water ice or a mixture of these materials. The roughness of the sea floors is smoother than that of terrain immediately surrounding the maria, consistent with sediment deposition throughout the observed sea floor.

5. Summary and implications

We analyzed the flyby T108 radar altimetry data acquired over Punga Mare and Baffin Sinus. The detection of the seafloor allowed us to investigate the liquid composition, the bathymetry, and seafloor topography of these liquid bodies. We found that the loss tangents of Punga Mare and Baffin Sinus are similar to that of Ligeia Mare within the 1-sigma uncertainty of the estimates ($\tan\delta = 4.4^{+0.9}_{-0.9} \times 10^{-5}$ for Ligeia Mare, $3^{+1}_{-1} \times 10^{-5}$ for Punga Mare and $3^{+1}_{-2} \times 10^{-5}$ for Baffin Sinus. See Supplementary Table 1 for relative composition values. However, the best fit values obtained here suggest that the composition for Punga Mare and Baffin Sinus might be most consistent with a binary methane-nitrogen system, with nitrogen approaching its solubility limit of 20% mole fraction in liquid methane and with little or no ethane or higher order hydrocarbons.

Several scenarios have been proposed which could permit ethane-poor seas. Mousis et al. (2016) and Choukroun et al. (2010) suggested that ethane might be sequestered by clathration if the crust of water ice or methane hydrates is exposed at the sea bed, resulting in methane-dominated liquids. However, this effect does not have any a priori latitude dependence.

The hydrological scenario proposed by Lorenz (2014) predicts an equator-to-pole gradation in methane and nitrogen abundance in the seas, much as salinity varies, e.g., between the Black Sea and the Mediterranean (or the Baltic and North Sea) on Earth. Higher inputs of 'fresh' liquid (on Titan, methane), either by higher rainfall rates and/or by larger land catchment areas, can displace solutes (salt, or ethane) to other basins in a system of connected seas. Although the simple model in Lorenz (2014) did not consider Punga specifically (at the time its hydraulic connection to the other seas was not obvious), the paradigm in that paper qualitatively suggests that the near-polar Punga Mare should be most ethane-poor, since circulation models suggest methane precipitation on Titan increases with latitude, and as the smallest sea, Punga Mare may have a proportionately larger catchment area, both factors favoring efficient flushing of solutes (the ethane and propane etc. which would predict higher loss tangents) into Kraken.

Alternatively, the latitudinal difference in composition could be explained as the results of the gradient in the surface temperature, assuming thermodynamic equilibrium with an atmosphere with constant methane mixing ratio (Tan et al., 2015; Tan and Kargel, 2018).

Particularly, using models of cryogenic chemical systems, Tan et al. (2015) suggested that latitudinal (e.g. two Kelvin difference in temperature from pole to 20 degrees of latitude) and seasonal variation of surface temperature could determine variations in vapor density and equilibrium phase compositions on Titan, thus affecting the atmospheric dynamics as well as the global fluid circulation in the surface and upper crust. More specifically, the authors predict more abundant but less dense liquid in large seas at higher latitude. These methane-rich liquids will tend to flow toward lower, warmer latitudes, re-equilibrating on the way to the equator with the lower atmosphere through evaporation of methane and thus a progressive enrichment of ethane at the lower latitude. Finally, ethane-richer, denser liquid would sink to the bottom of the sea and then flow poleward in a density-controlled cycle analogous to thermohaline circulation systems on Earth (Tan et al., 2015). However this thermally-driven local-thermodynamic equilibrium circulation scenario, fails to predict the compositions we have observed, but rather is too ethane-rich in the northern seas. These models also predict the presence of higher order components, such as propane, which would further increase absorptivity and likely make the models incompatible with observed loss tangents. Based on these observations, it appears that non-equilibrium processes are key to understanding Titan, as on Earth, where the atmospheric humidity is not 100% despite being a largely water-covered planet.

Given that the loss tangents obtained so far are the same in a formal (one sigma) sense, it may in fact be challenging to properly infer any compositional variability of seas until the composition and depth of Kraken Mare, by far the largest liquid reservoir, are determined.

To better constrain the uncertainties regarding this variability, new orbital missions equipped with multi-frequency radar dedicated to map composition of Titan seas and lakes are envisaged. Additionally, direct measurements of composition and dielectric properties by one or more in-situ probes (Lorenz and Mann, 2015) could provide ground truth to robustly infer composition globally from radar data. Therefore, a combination of orbital data along with in situ direct measurements would represent the most efficient exploration effort.

While this effort requires future missions (orbital or landed) to Titan, it is remarkable that the Cassini mission (and its radar in particular), although not conceived for such measurements, has been able to obtain depths and bulk liquid compositions of lakes and seas with only a handful of observations.

Acknowledgements

M.M. and R.S. would like to acknowledge support from Italian Space Agency (ASI) grant 2014-041-R.0; G.D.A. was supported by the Italian Ministry of University and Research through FIRB-RBFR130ICQ grant. M.M., A.G.H., and V.P. would like to acknowledge support from NASA CDAP grant NNX15AH10G; R.L. acknowledges NASA grants NNX13AH14G and NNX13AK97G. J.I.L. is grateful for the ministrations of the Cassini mission in supporting his research. We appreciate the efforts of the Cassini TOST (Titan Orbiter Science Team) and RADAR Team in planning and executing these observations, in particular Yanhua Anderson and Richard West took great care to implement the spacecraft turns and instrument settings to achieve the Punga inspection reported here.

Appendix A. Supplementary material

Supplementary material related to this article can be found online at https://doi.org/10.1016/j.epsl.2018.05.033.

References

Alberti, G., Festa, L., Papa, C., Vingione, G., 2009. A waveform model for near-Nadir radar altimetry applied to the Cassini mission to Titan. IEEE Trans. Geosci. Remote Sens. 47 (7), 2252–2261. https://doi.org/10.1109/TGRS.2009.2012718.

Barnes, J.W., Sotin, C., Soderblom, J.M., et al., 2014. Planet. Sci. 3 (3). https://doi.org/10.1186/s13535-014-0003-4.

Blackman, R.B., Tukey, J.W., 1959. Particular pairs of windows. In: The Measurement of Power Spectra, from the Point of View of Communications Engineering. Dover, New York, pp. 98–99.

Birch, S.P.D., Hayes, A.G., Dietrich, W.E., Howard, A.D., Bristow, C.S., Malaska, M.J., Lopes, R.M.C., 2017. Geomorphologic mapping of Titan's polar terrains: constraining surface processes and landscape evolution. Icarus 282, 214–236. https://doi.org/10.1016/j.icarus.2016.08.003.

Born, M., Wolf, E., 1999. Principles of Optics: Electromagnetic Theory of Propagation, Interference and Diffraction of Light, 7th ed. Cambridge University Press. ISBN 0-521-64222-1, section 2.3.3.

Cheung, H., Wang, D.I.-J., 1964. Solubility of volatile gases in hydrocarbon solvents at cryogenic temperatures. Ind. Eng. Chem. Fundam. 3 (4), 355–361. https://doi.org/10.1021/i160012a014.

Choukroun, M., Grasset, O., Tobie, G., Sotin, C., 2010. Stability of methane clathrate hydrates under pressure: influence on outgassing processes of methane on Titan. Icarus 205 (2), 581–593. https://doi.org/10.1016/j.icarus.2009.08.011.

Cuomo, K.M., 1992. A Bandwidth Extrapolation Technique for Improved Range Resolution of Coherent Radar Data. Project Report CJP-60, Revision 1, MIT Lincoln Laboratory.

Elachi, C., et al., 2004. Radar: the Cassini Titan radar mapper. Space Sci. Rev. 115 (1), 71–110. Available http://link.springer.com/article/10.1007%2Fs11214-004-1438-9 [Online].

Grima, C., Mastrogiuseppe, M., Hayes, A.G., Wall, D.S., Lorenz, R.D., Hofgartner, J.D., Stiles, B., Elachi, C., 2017. Surface roughness of Titan's hydrocarbon seas. Earth Planet. Sci. Lett. (ISSN 0012-821X) 474, 20–24. https://doi.org/10.1016/j.epsl.2017.06.007.

Hayes, A.G., 2016. The lakes and seas of Titan. Ann. Rev. Earth Space Sci. 44 (1), 57–83.

Hayes, A.G., Aharonson, O., Callahan, P., Elachi, C., Gim, Y., Kirk, R., Lewis, K., Lopes, R., Lorenz, R., Lunine, J., Mitchell, K., Mitri, G., Stofan, E., Wall, S., 2008. Hydrocarbon lakes on Titan: distribution and interaction with a porous regolith. Geophys. Res. Lett. 35, 9204.

Hayes, A.G., Lorenz, R.D., Donelan, M.A., Manga, M., Lunine, J.I., Schneider, T., Lamb, M.P., Mitchell, J.M., Fischer, W.W., Graves, S.D., Tolman, H.L., Aharonson, O., Encrenaz, P.J., Ventura, B., Casarano, D., Notarnicola, C., 2013. Wind driven capillary-gravity waves on Titan's lakes: hard to detect or non-existent? Icarus (ISSN 0019-1035) 225 (1), 403–412. https://doi.org/10.1016/j.icarus.2013.04.004.

Hayes, A.G., Birch, S.P.D., Dietrich, W.E., Howard, A.D., Kirk, R.L., Poggiali, V., Mastrogiuseppe, M., Michaelides, R.J., Corlies, P.M., Moore, J.M., Malaska, M.J., Mitchell, K.L., Lorenz, R.D., Wood, C.A., 2017. Topographic constraints on the evolution and connectivity of Titan's lacustrine basins. Geophys. Res. Lett. 44 (23), 11745–11753. https://doi.org/10.1002/2017GL075468.

Iess, L., et al., 2012. The tides of Titan. Science 337, 457. https://doi.org/10.1126/science.1219631.

Janssen, M.A., Le Gall, A., Lopes, R.M., Lorenz, R.D., Malaska, M.J., Hayes, A.G., Neish, C.D., Solomonidou, A., Mitchell, K.L., Radebaugh, J., Keihm, S.J., Choukroun, M., Leyrat, C., Encrenaz, P.J., Mastrogiuseppe, M., 2016. Titan's surface at 2.18-cm wavelength imaged by the Cassini RADAR radiometer: results and interpretations through the first ten years of observation. Icarus (ISSN 0019-1035) 270, 443–459. https://doi.org/10.1016/j.icarus.2015.09.027.

Le Gall, A., et al., 2016. Composition, seasonal change, and bathymetry of Ligeia Mare, Titan, derived from its microwave thermal emission. J. Geophys. Res., Planets 121, 233–251. https://doi.org/10.1002/2015JE004920.

Lopes, R.M.C., et al., 2013. Cryovolcanism on Titan: new results from Cassini RADAR and VIMS. J. Geophys. Res., Planets 118, 416–435. https://doi.org/10.1002/jgre.20062.

Lorenz, R.D., 2014. The flushing of Ligeia: composition variations across Titan's seas in a simple hydrological model. Geophys. Res. Lett. 41, 5764–5770. https://doi.org/10.1002/2014GL061133.

Lorenz, R.D., Mann, J., 2015. Seakeeping on Ligeia Mare: dynamic response of a floating capsule to waves on the hydrocarbon seas of Saturn's moon Titan. Johns Hopkins APL Tech. Dig. 33 (2), 82–94.

Malaska, M.J., Hodyss, R., Lunine, J.I., Hayes, A.H., Hofgartner, J.D., Hollyday, G., Lorenz, R.D., 2017. Laboratory measurements of nitrogen dissolution in Titan lake fluids. Icarus (ISSN 0019-1035) 289, 94–105. https://doi.org/10.1016/j.icarus.2017.01.033.

Mastrogiuseppe, M., et al., 2014a. The bathymetry of a Titan sea. Geophys. Res. Lett. 41, 1432–1437. https://doi.org/10.1002/2013GL058618.

Mastrogiuseppe, M., et al., 2014b. Titan dune heights retrieval by using Cassini radar altimeter. Icarus (ISSN 0019-1035) 230, 191–197. https://doi.org/10.1016/j.icarus.2013.09.028.

Mastrogiuseppe, M., et al., 2016. Radar sounding using the Cassini altimeter: waveform modeling and Monte Carlo approach for data inversion of observations of Titan's seas. IEEE Trans. Geosci. Remote Sens. 54 (10). https://doi.org/10.1109/TGRS.2016.2563426.

Mastrogiuseppe, M., et al., 2018. Bathymetry and composition of Titan's Ontario Lacus derived from Monte Carlo-based waveform inversion of Cassini RADAR altimetry data. Icarus (ISSN 0019-1035) 300, 203–209. https://doi.org/10.1016/j.icarus.2017.09.009.

Mitchell, K.L., Barmatz, M.B., Jamieson, C.S., Lorenz, R.D., Lunine, J.I., 2015. Laboratory measurements of cryogenic liquid alkane microwave absorptivity and implications for the composition of Ligeia Mare, Titan. Geophys. Res. Lett. 42, 1340–1345. https://doi.org/10.1002/2014GL059475.

Mitri, G., Bland, M.T., Showman, A.P., Radebaugh, J., Stiles, B., Lopes, R.M.C., Lunine, J.I., Pappalardo, R.T., 2010. Mountains on Titan: modeling and observations. J. Geophys. Res. 115, E10002. https://doi.org/10.1029/2010JE003592.

Mousis, O., Lunine, J.I., Hayes, A.G., Hofgartner, J.D., 2016. The fate of ethane in Titan's hydrocarbon lakes and seas. Icarus 270, 37–40. https://doi.org/10.1016/j.icarus.2015.06.024.

Poggiali, V., et al., 2016. Liquid-filled canyons on Titan. Geophys. Res. Lett. 43, 7887–7894. https://doi.org/10.1002/2016GL069679.

Radebaugh, J., et al., 2007. Mountains on Titan observed by Cassini Radar. Icarus (ISSN 0019-1035) 192 (1), 77–91. https://doi.org/10.1016/j.icarus.2007.06.020.

Stofan, E.R., et al., 2007. The lakes of Titan. Nature 445, 61–64. Available http://www.nature.com/nature/journal/v445/n7123/abs/nature05438.html [Online].

Tan, S.P., Kargel, J.S., 2018. Multiphase-equilibria analysis: application in modeling the atmospheric and lacustrine chemical systems of Saturn's moon Titan. Fluid Phase Equilib. (ISSN 0378-3812) 458, 153–169. https://doi.org/10.1016/j.fluid.2017.11.020.

Tan, S.P., Kargel, J.S., Jennings, D.E., Mastrogiuseppe, M., Adidharma, H., Marion, G.M., 2015. Titan's liquids: exotic behavior and its implications on global fluid circulation. Icarus (ISSN 0019-1035) 250, 64–75. https://doi.org/10.1016/j.icarus.2014.11.029.

Ulaby, F.T., Moore, R.K., Fung, A.K., 1982. Microwave Remote Sensing, vol. 2. Addison–Wesley, Reading, MA (Chapters 11 and 12).

West, R.D., et al., 2009. Cassini RADAR sequence planning and instrument performance. IEEE Trans. Geosci. Remote Sens. 47 (6), 1777–1795. https://doi.org/10.1109/TGRS.2008.2007217.

Wood, C.A., et al., 2010. Impact craters on Titan. Icarus (ISSN 0019-1035) 206 (1), 334–344. https://doi.org/10.1016/j.icarus.2009.08.021.